Atmos. Chem. Phys. Discuss., 10, 7507–7552, 2010
www.atmos-chem-phys-discuss.net/10/7507/2010/

Atmospheric Chemistry and Physics Discussions

This discussion paper is/has been under review for the journal Atmospheric Chemistry and Physics (ACP). Please refer to the corresponding final paper in ACP if available.

The influence of biomass burning on tropospheric composition over the tropical Atlantic Ocean and Equatorial Africa during the West African monsoon in 2006

J. E. Williams[1], M. P. Scheele[1], P. F. J. van Velthoven[1], V. Thouret[2,3], M. Saunois[2,3,*], C. E. Reeves[4], and J.-P. Cammas[2,3]

[1]Royal Netherlands Meteorological Institute, De Bilt, The Netherlands
[2]Université de Toulouse, UPS, LA(Laboratorie d'Aerologie), 31400 Toulouse, France
[3]Laboratorie d'Aeronomie, (UMR UPS/CNRS 5560), Observatoire Midi-Pyrénées, Toulouse, France
[4]School of Environmental Sciences, University of East Anglia, Norwich, UK

* now at: National Center for Atmospheric Research, Boulder, CO, USA

Received: 2 December 2009 – Accepted: 11 March 2010 – Published: 23 March 2010

Correspondence to: J. E. Williams (williams@knmi.nl)

Published by Copernicus Publications on behalf of the European Geosciences Union.

Abstract

We have performed simulations using a 3-D global chemistry-transport model (TM4_AMMA) to investigate the effect that continental transport of biomass burning plumes have on regional air quality over Equatorial Africa during the West African Monsoon (WAM) period in 2006. By performing a number of sensitivity studies we show that biomass burning emissions from southern Africa (0–40° S) have a strong influence on the composition of the tropical troposphere around Equatorial Africa and the outflow regions towards the west, especially between 10° S–10° N. By altering both the temporal distribution and the injection heights used for introducing the biomass burning emissions we show that changes in temporal distribution are much more important in determining the daily variability of trace gas species over the southern Atlantic than boundary layer processes. When adopting the GFEDv2 emission inventory the maximum concentrations in CO and O_3 occur between 0–5° S, which coincides with the position of the southern African Easterly Jet. By comparing co-located model output with in-situ measurements made during the AMMA measurement campaign we show that the model fails to capture the tropospheric profile of CO in the burning region, as well as the "extreme" concentrations of both CO and O_3 seen around 600–700 hPa above Equatorial Africa. Trajectory analysis show that the 6-hourly ECMWF meteorological fields do not allow transport of biomass burning plumes from southern Africa directly into the mid-troposphere around ~6° N. Similar trajectory simulations repeated using an updated meteorological dataset, which assimilates additional measurement data for the African region, shows markedly different origins for pollution events and reveals that the performance of the CTM is heavily constrained by the ECMWF operational analysis data which drives the model.

ACPD

10, 7507–7552, 2010

1 Introduction

The emission of gaseous and particulate matter from both human induced biomass burning (BB) and (natural) wildfires has been identified as the most dominant source of CO, NO_x (= NO + NO_2), Non-Methane Hydrocarbons (NMHCs), SO_2 and aerosol particles in sparsely populated regions (Crutzen and Andreae, 1990; Andreae and Merlet, 2001). A dominant region where such fires occur is the African continent (e.g. Jain, 2007), where the seasonality of the burning practices results in two distinctive emission phases, one occurring in the Northern Hemisphere (NH), between 0–20° N, and one in the Southern Hemisphere (SH), between 5–20° S. These typically occur between December to March and June to September, for the NH and SH, respectively. Moreover, the intensity of fires and the total area burnt exhibit a large degree of interannual variability with respect to the seasonal cycle (e.g. Giglio et al., 2006; van der Werf et al., 2006). This introduces a certain degree of uncertainty when assessing the total regional emissions from such events for any particular year. As climate changes, such events are likely to increase in both intensity and frequency in Africa (Intergovernmental Panel on Climate Change, 2007). Hence, the importance of such emission sources for the tropics will potentially be enhanced in the coming decades providing motivation to investigate whether large-scale atmospheric models can capture the variability in tropospheric composition which has been observed in the African region (e.g. Sauvage et al., 2007).

For long-lived trace gases such as CO, pyrogenic convection into the free troposphere results in polluted air-masses traveling long distances (e.g. Staudt et al., 2002; Edwards et al., 2006), where signatures of such events have previously been observed in measurements made around Africa (e.g. Muhle et al., 2002; Hobbs et al., 2003). Another important trace species linked to BB is tropospheric ozone (O_3), which is formed via the photochemical oxidation of NO_2 released during burning events. For instance, it has previously been shown that enhanced concentrations of tropospheric O_3 in the lower atmosphere over Equatorial Africa (EA) during July can be attributed directly to

ACPD
10, 7507–7552, 2010

emissions from fires near the equator (Sauvage et al., 2005; Sauvage et al., 2007). Moreover, recent aircraft (Reeves et al., 2010; Andrés-Hernàndez et al., 2009) and ozone sonde measurements (Thouret et al., 2009) taken as part of the African Monsoon Multidisciplinary Analysis (AMMA, www.amma-eu.org; Redelsperger et al., 2006) have also shown enhancements in both CO and O_3 at around 4–5 km, especially during August 2006 near the coast of Nigeria, Benin and Ghana. As part of AMMA, these enhancements have recently been found to be influenced by BB activity in southern Africa (Real et al., 2009), as well as other emission sources in the Guinea region (Ancellet et al., 2009). However, the transport of such polluted air-masses towards EA is not continuous during the WAM, as demonstrated by Mari et al. (2008). They found that during the "break" phase of the southern African Easterly Jet (AEJ-S) between the 3–8 August 2006, polluted air-masses were directed back over the continent rather than westwards out over the tropical Atlantic Ocean.

A recent intercomparison study involving a set of global CTMs has shown that several large-scale models have difficulty in capturing the correct distribution of tropospheric O_3 over EA during the WAM (Williams et al., 2010) as compared with both ozone sonde profiles and a composite of aircraft measurements made during AMMA. The ability of the CTMs to capture the continental transport of such pollutants is dependent on various model components, such as the chemical mechanism, the convective parameterization, the quality of the meteorological data used to drive the model and the accuracy of the BB emission dataset used to introduce such events. Moreover, the lofting of the resulting emissions due to the increased buoyancy of the hot air from the burning process significantly increases injection heights (e.g. Kahn et al., 2007; Labonne et al., 2007), thus having the potential to affect long-range transport. However, recent sensitivity studies performed with CTM's investigating the effect of boreal fire emissions on air quality in North America are somewhat inconclusive concerning injection heights. Some of these studies have found this parameter to be important (e.g. Colarco et al., 2004; Leung et al., 2007; Turquety et al., 2007), whereas others place more emphasis on the temporal variability in the emission dataset employed (Chen et

al., 2009). The present study contributes towards this debate by examining the effects of various model parameters on simulating the transport of BB plumes out of southern Africa and the chemical processing within such plumes near EA during the WAM. Indeed this region exhibits unique meteorological behaviour (Nicholson and Grist, 2003) in conjunction with high BB intensity during the season June-July-August (JJA), which introduces different conditions compared to the regions used in the previous studies.

In Sect. 2 we describe the model configuration used and the sensitivity studies that have been performed for this study. In Sect. 3 we highlight the differences in the monthly variability in the concentrations of CO and O_3 (hereafter referred to as [CO] and [O_3], respectively) over the Gulf of Guinea that occur between the various sensitivity studies, and examine the effects of altering model parameters associated with introducing BB into the CTM. In Sect. 4 we compare co-located model output against a host of different in-situ measurement data relevant for the lower to mid troposphere to assess the performance of the model and examine which model parameters have the largest influence. In Sect. 5 we present trajectory analyses to determine the origin of air entering the AMMA measurement region during the WAM and finally, in Sect 6, we present our conclusions and make recommendations for future studies.

2 Model description

2.1 Experimental set up

The global CTM used in this study is the TM4_AMMA model, which adopts a horizontal resolution of $3^{\circ}\times2^{\circ}$, has 34 vertical levels up to 0.1 hPa and is driven by 6 hourly European Centre for Medium range Weather Forecasting (ECMWF) meteorological analysis data. The main features are described in Williams et al. (2009a), apart from a small number of modifications, of which a brief summary is given here. The heterogeneous rate data used for accounting for the scavenging of soluble trace gases into cloud droplets has been updated, where wet deposition is now also included for

both methylglyoxal and the lumped aldehyde tracer that is included in the modified CBM4 mechanism to account for higher aldehydes (C2 and above, Houweling et al., 1998). The parameterization of Heymsfield and McFarquar (1996) has been included for the description of the microphysical properties of cirrus particles which provides the available cross sectional area of the ice particle field for all grid cells containing ice water content above 10^{-10} kg m^{-3}. This cross sectional area is subsequently converted into a surface area density (cm^2/cm^3) using a scaling ratio of 10, which has recently been estimated for non-homogenous randomly shaped particles (Schmitt and Heymsfield, 2005). The effective radius of the ice particles is calculated by using the cross-sectional area in the parameterization of Fu (1996), which has been validated against data from a number of different measurement campaigns both in the tropics and mid-latitudes (Heymsfield, 2003). These parameterizations replace the fixed ice particle size of 50 µm previously included in TM4_AMMA. The corresponding surface area density available from cloud droplets has also been modified using a fixed cloud droplet radius of 8 µm. These micro-physical properties for these particles are then used for calculating the conversion of N_2O_5 into HNO_3 on both types of surface according to the approach outlined in Jacob (2000). This improvement in the description of the available surface area density and an update of the relevant uptake parameters has been shown to reduce the heterogeneous conversion of N_2O_5 compared to the fixed values adopted in the previous version of TM4_AMMA, leading to increases in annual means of mid to upper tropospheric [O_3] of between ~3–5% and [NO_3] of between ~25–50% (Williams et al., 2009b).

For the anthropogenic and biomass burning emissions we retain the inventories from the EU project entitled "Reanalysis of the TROpospheric chemical composition over the past 40 years" (RETRO, http://retro.enes.org/) and the Global Fire Emissions Database version 2 (GFEDv2, van der Werf et al., 2006) as used in Williams et al. (2009a). Due to the NH_3 emissions being currently unavailable from the GFEDv2 dataset we adopt the 5-year average for the period 1998–2002 from the GFEDv1 dataset as used in recent intercomparison studies (Stevenson et al., 2006). For this study, we modified the

application of the BB emissions in the tropics between 20° N–20° S by increasing the maximum injection height to 2 km as suggested by recent satellite observations of BB plumes (Labonne et al., 2007). This results in ∼50% of the emissions being injected between 0–1 km and ∼50% being injected between 1–2 km. Moreover, the tropical BB emissions are given a daily cycle to mimic the increased burning in the afternoon, which has been observed from a combination of different satellite instruments that have staggered overpass times (e.g. Boersma et al., 2008) and geo-stationary platforms (e.g. Giglio, 2007; Roberts et al., 2009). Placing such a constraint on the daily emissions has been found to be important with respect to capturing (e.g.) the correct distribution of CO in the lower troposphere (LT) (see e.g. Chen et al., 2009).

2.2 Definition of the sensitivity studies

Here we define a number of sensitivity studies for the purpose of quantifying the importance that regional BB emissions from Africa have on the composition of the LT over (near) the Gulf of Guinea during the WAM. Moreover, we also assess the influence of altering the vertical and temporal distribution of BB emissions on the long-range transport of pollutants out of the African continent by adopting different approaches for introducing such emissions into TM4_AMMA. An overview of the complete set of simulations included in the study is given in Table 1. The baseline simulation (hereafter referred to as FULL) applies BB emissions for all regions using monthly averaged emission inventories from the GFEDv2 database (van der Werf, 2006). Two further simulations are defined where we turn off all BB emissions sequentially from southern Africa (40° S–0° N, 20° W–40° E) and Guinea (0–10° N, 20° W–40° E) (hereafter referred to as NOSAFR and NOGUIN, respectively), where the seasonality exhibited in the GFEDv2 BB emission inventory for these two regions is similar to that shown in Bian et al. (2007) (i.e. peaks in the BB emissions occur in February and September for the NH and SH, respectively). For the Sahel (10° N–20° N) and the Sahara (20° N–40° N) regions, the annual BB emission fluxes are low therefore their influence is assumed to be negligible during the WAM. The trace gases whose emission fluxes are subsequently reduced

when turning BB emissions off are CO, NO_x, NMHCs, SO_2 and NH_3.

To explore the effect of temporal variability of the BB emission fluxes, a simulation is performed using the GFEDv2 8-day emission inventory (van der Werf et al., 2006) (hereafter referred to as FULL_8day), where the flux estimates are updated every 8 days resulting in changes to the BB emission fluxes 3–4 times every month. Moreover, the cumulative sum which is introduced into the model between the monthly and 8-day GFEDv2 inventories may be slightly different as a result of coarsening from the $1^\circ \times 1^\circ$ on which the inventory is provided onto the horizontal grid of $3^\circ \times 2^\circ$ defined in TM4_AMMA.

To investigate the sensitivity of long-range transport and in-situ O_3 formation on the injection height of the BB emissions, we define a simulation where the maximum injection height is doubled compared to the FULL simulation (hereafter referred to as HIGH_IH). HIGH_IH places 50% of the emissions between 0–2 km, ~25% between the 2–3 km and ~25% between the 3–4 km, similar to the recommendations by Lavoue et al. (2000) for sub-tropical regions. Moreover, these heights are all typically still within the boundary layer over tropical BB regions as suggested by Labonne et al. (2007) for southern Africa, where the application of the daily cycle ensures that the boundary layer height is well developed when the majority of the emissions are injected (in the afternoon).

Since the estimation of CO emissions from BB depends on the methodology and type of data product used, significant uncertainties exist between different inventories (e.g. Ito and Penner, 2005; Monks et al., 2009). We therefore define another sensitivity test where the emission of CO from BB is increased by 50% in southern Africa during JJA in order to increase its atmospheric lifetime during the WAM (hereafter referred to as HIGH_CO). This results in an increase of 21.6 Tg CO over the season for 2006.

Finally, we define a simulation where we increase the anthropogenic emissions released in Africa by 8.4% to account for the rapid growth of urban conurbations since 2000 (hereafter referred to as HIGH_ANTH). The annual growth rate in anthropogenic emissions is highly uncertain due to the lack of accurate emission data therefore an in-

crease of 1.4% per year for African cities is used as observed from the increase in NO_x for Cairo (van der A et al., 2008). This leads to increases in CO and NO_x of 0.78 Tg CO and 7.4×10^{-2} Tg N for JJA, respectively.

3 The influence of regional biomass burning on tropospheric composition between 3° W–6° E

In this study we utilize the same 2-D cross section adopted for the AMMA Model Intercomparison Project (AMMA-MIP, Williams et al., 2010), which contains averages of tracer concentrations between 3° W–6° E for a latitude range of 20° S–40° N. This 2D cross section includes the Cotonou measurement site (6.2° N, 2.2° E), at which ozonesonde observations were made during 2005 and 2006 (Thouret et al., 2009), and also the location where instrumented aircraft flights were conducted during the AMMA measurement campaign (e.g. Reeves et al. 2010). The tracer fields are written out every three hours, which are then averaged to produce both monthly and daily values for the analysis presented here. In order to differentiate between air that originates from southern Africa, local convection and the background we also included a set of chemically passive tracers. These "region" tracers are given a fixed atmospheric lifetime of 20 days, where concentrations are fixed at 100 pptv below 850 hPa (over land) for both of the regions used in the study. For grid cells which contain both land and ocean a scaling is applied, where the fixed concentration is weighted with the land fraction. By correlating "peaks" in CO and O_3 with the respective passive tracers we examine the variability of transport into the region to determine whether using 6-hourly updates of the meteorological fields is sufficient.

3.1 Monthly comparisons

Figures 1 and 2 show the distribution of tropospheric CO and O_3 in the 2-D cross-section for the FULL simulation, along with the percentage differences calculated for

both the NOGUIN and NOSAFR simulations for each month during JJA, respectively. Examining the tropospheric distribution in the FULL run for both CO and O_3 it can be seen that the maximum values typically occur around 0–5° S between 700–850 hPa for both trace species. This maximum has been shown to occur at similar locations for a range of different CTM's which employ various combinations of parameterizations for convective and advective transport processes, different chemical schemes and a different BB emission inventory (Williams et al., 2010). The location of this maximum corresponds to the mean position of the AEJ-S for this year as shown in Mari et al. (2008).

Analysis of the emission budgets during JJA for the tropics and subtropics (calculated as the emission released between 34° N–34° S across all longitudes) shows that the NOGUIN (NOSAFR) simulation exhibits reductions of ~0.4% (~17.5%) in emitted CO, ~<0.1% (~5.8%) in NO_x, ~0.2% (~0.3%) in NMHC and very small differences in both SO_2 and NH_3. This causes reductions in the tropical tropospheric burdens of CO and O_3 below 500 hPa of ~1.4% (~7.5%) and ~0.3% (~3.2%), respectively, where the longer atmospheric lifetime of CO means there is an effect from the proceeding months. In part, the reduction in the in-situ formation of tropospheric O_3 is due to a decrease in resident [NO_2] of between ~50–60% (not shown) due to suppressed [PAN]. The corresponding difference plots demonstrate that ~40–50% of the maximum values of CO and O_3 in the 2-D transect occur as a direct result of BB emissions from southern Africa, where the most significant effects occur in the LT below 500 hPa. It can be seen that the influence of BB from southern Africa extends far inland over West Africa reaching ~15° N, thus influencing the southern coast and well into the Sahel region (see Sect. 4), although the largest differences occur between 5° S–5° N. Thus, BB emissions from southern Africa have a strong influence on the oxidative capacity of the troposphere over EA (where [OH] is typically governed by [O_3]), especially for the LT.

For the FULL_8day simulation (not shown) we found a net decrease in the emission of CO and NO_x between 34° N–34° S (0–34° S) of ~6% (~10%) and ~1.6% (~3.5%),

ACPD
10, 7507–7552, 2010

respectively. Comparing the corresponding monthly means between the FULL_8day simulation and the FULL simulation revealed that the differences in both [CO] and [O_3] are limited to <10% and change throughout JJA. For brevity we refer the reader to the next section where we show direct comparisons between the two simulations and to Sect. 4, where further details are provided.

3.2 Daily mean variations between 20° N and 20° S

Figure 3 shows Hovmöller diagrams of the daily means of [CO] and [O_3] along the 2D north-south transect during JJA at 650hPa, which corresponds to where the largest variability occurs in the O_3 observations (see next section). Each daily mean is an average taken between 3° W–6° E. This illustrates the intermittent character of CO and O_3 around EA. Figures 4a and b show the variability in the daily mean mixing ratio for the same trace gas species for the various sensitivity simulations for 4–6° S and 6–8° N at ~860 hPa and ~670 hPa, respectively. These two latitudinal averages were selected (i) to correspond to the region where the maximal concentrations for both [CO] and [O_3] occur, as shown in Figs. 1 and 2, and (ii) to be directly over the Cotonou measurement site from which ozone sondes were launched, as well as corresponding to the region where selected flights from the BAe-146 aircraft occurred during the AMMA measurement campaign. The two selected altitudes are representative of the LT and the middle troposphere (MT), where the "extreme" [O_3] was observed (Thouret et al., 2009).

When combined, Figs. 3 and 4 exemplify the large fluctuations that occur in the daily values of these trace species, and that are most pronounced in the SH. Moreover, the top right panels of Fig. 3 demonstrate unambiguously that BB emissions from southern Africa cause the large fluctuations and dominate the composition of the tropical troposphere in the 2-D transect for this season. This is in agreement with previous findings in the literature regarding the effects of BB on this region (e.g.) Sauvage et al. (2006). In Fig. 4, a high correlation is seen between the variability in the southern Africa passive tracer (S_Afr) and CO for both locations, where the "pulsing" effect occurs due to variations in the transport of air from southern Africa. Moreover, the "break" period identified

by Mari et al. (2008) can also be clearly seen in [CO] and [S_Afr] between 3–8 August (Julian Days (JD) 215–222), as well other periods during July. For BB emissions from the Guinea region the most important differences occur during August in the SH, in line with the differences shown in (e.g.) Fig. 2.

For the simulation which adopts the 8-day inventory (FULL_8day), the leftmost panels of Fig. 3 show that there are generally increases in both [CO] and [O_3] in the SH as compared with those that adopt the monthly inventory (FULL), with the notable exception of 29 July–3 August (JD 210–215) around 10–20° S. Figure 4a shows that at lower altitudes the daily mean values change as the season progresses, where higher (lower) concentrations are seen in the FULL run for June (August). For the HIGH_IH run, the increased injection height results in a marginal increase in [CO] being transported out of the source region in the SH (e.g. around JD 220) when compared to the FULL_8day simulation. Altering the temporal variability of emissions from monthly to 8-day averages introduces a much larger effect than increasing the injection height, supporting the conclusions of Chen et al. (2009).

Analysis of the chemical budgets shows that the annual tropical tropospheric CO (O_3) burden increases (decreases) by 3.5% (1%) compared to the FULL_8DAY run as a result of using the enhanced injection heights. Hence it is still a non-negligible effect although such injection heights would not be applicable to all burning events and therefore the result should be considered a maximal effect. Comparing the distribution of CO in Fig. 3 for the FULL, FULL_8day and HIGH_IH runs against the composite assembled from the Measurements Of Pollution In The Troposphere (MOPITT) instrument shown in Mari et al. (2008) reveals that the location of the maximum [CO] in TM4_AMMA simulations does not extend far enough northward over the Equator, regardless of the changes in the temporal or vertical distribution of the BB emissions. However, the increase in [CO] between July and August observed by MOPITT is captured by the model indicating that the seasonality of the GFEDv2 monthly and 8-day inventories seems to be correct, and that the applied meteorological analyses from ECMWF may have problems in positioning the meteorological equator correctly with

respect to latitude. For instance, recent assimilation of soundings taken as part of the AMMA campaign into ECMWF analyses results in the AEJ-S being shifted northwards due to modification of the wind fields (Agusti-Panareda et al., 2009) which would help to improve the comparison of [CO] in the MT presented here. We expand the discussion on this in Sect. 5.

Finally, the HIGH_CO run shows that a significant increase occurs for [CO] as would be expected considering the increase in the BB emission flux. This increase extends into West Africa (6–8° N), where an increase in the background concentration occurs for CO especially for the LT (see Sect. 4.2). However, at ~650 hPa this increase in CO does not extend the transport northwards, resulting in no significant improvement with the MOPITT composite shown in Mari et al. (2008). For [O_3] corresponding decreases occur in the SH (see JD 210), whereas in the NH the differences are rather negligible.

4 Measurements against model results

Here we compare co-located model output against a host of different in-situ measurements representative of the LT in both Equatorial and southern Africa during the period of interest. The aim is to assess possible short-comings in the model performance for Africa near source regions and for locations influenced by long-rang transport of BB plumes, as well as to investigate whether the daily and monthly variability can be captured with a large-scale CTM. Moreover, we also assess some improvements due to the model modifications by comparing the sensitivity studies.

4.1 Regional comparisons in southern Africa

During 2006 the MOZAIC program (Measurement of OZone, water vapour, carbon monoxide and nitrogen oxides by airbus in-service AIrCraft) measured tropospheric profiles of [CO] and [O_3] during take-off and landing of passenger aircraft from Windhoek, Namibia (22.5° S, 17.5° E). Measurements were made during both day and night

thus (partly) capturing the effects of the daily cycle imposed on the BB activity and diurnal variations in photochemical activity. Figure 5 shows the monthly mean comparisons of tropospheric [CO] between the MOZAIC measurements and the different simulations for June, July and August. The top three figures relate to simulations performed using the monthly inventory and the lower three figures using the 8-day inventory. Comparing the 1-σ variability associated with the measurements (green lines) for each month shows that the variability in the LT increases as the regional BB activity increases. The comparison to model results shows that there is a significant under prediction of tropospheric CO at Windhoek by the model during the entire season. Similar comparisons made for seasons March-April-May (MAM) (September-October-November (SON)) (not shown) result in smaller (larger) discrepancies for CO than for JJA, in line with the changes in the intensity of the seasonal BB cycle in southern Africa. These seasonal differences provide evidence that the discrepancy is probably due to either the seasonal emission of CO in southern Africa in the BB inventory not being optimal, that the temporal and/or geographical distribution is not accurate or that there is a missing source term in the model such as additional biogenic production. Although we have shown that increasing the total flux improves the agreement significantly in July (bottom middle panel of Fig. 5), it is not possible to give a detailed quantification of the importance of each of these potential causes in the current study. Moreover, it should be noted that we find that increasing the CO flux across the entire region degrades comparisons in EA (see Sect. 4.2).

The NOSAFR run in Fig. 5 shows that emissions from regional BB sources account for ~25% of the CO in the LT at Windhoek, meaning ~75% occurs as a result of other emission sources (e.g. nearby urban centers), in-situ chemical formation (e.g. HCHO photolysis) and long-range transport (e.g. from South America). Comparing the FULL_8day simulation shows that there is a decrease in the monthly mean [CO] for the lower levels by a few ppbv, thus slightly degrading the quality of the comparisons. For the HIGH_IH simulation increases of a few percent occur in the MT between 600–750 hPa. Finally, the HIGH_CO run leads to a significant improvement in the agreement

ACPD
10, 7507–7552, 2010

below 600 hPa for all months shown. The similarity in the CO profiles of the different model simulations above 600hPa reveals that this increase is limited to the LT. An additional comparison performed using the output from the TM5 model (Krol et al., 2005) ran in zoomed mode (1°×1°) over Africa using 3 hourly ECMWF meteorological data also did not show any significant improvement in the quality of the comparison for these MOZAIC profiles (V. Huijnen, personal communication, 2009). Therefore the coarsening of the BB emission inventory onto the 3°×2° grid adopted in this study and the update frequency of the wind fields do not seem to be important contributing factors towards the disagreement shown in Fig. 5. In summary, the improvements shown in the comparisons of the tropospheric profiles for the HIGH_CO run again provide strong evidence that the emission of CO from southern Africa is too low during 2006.

When performing similar comparisons against the corresponding tropospheric O_3 profiles from the MOZAIC database the agreement is much better (c.f. Fig. 8 in Williams et al., 2009a). For all months during JJA, the NOSAFR run under-predicts tropospheric [O_3] in the lower atmosphere by ~5 ppbv (~15% of that which is measured), whereas the FULL simulation tends to over-predict for July and August by a few ppbv, although the profile shape is captured quite well. Comparing the FULL_8day simulation shows that there is only a marginally better agreement with the observations. Although the agreement for O_3 is also dependent on the chemical mechanism employed, this suggests that for NO_x the BB emission estimates provided in the GFEDv2 inventory are rather good for this year and do not need to be increased as with CO. For the other sensitivity studies no significant differences occur compared to the FULL_8day run, apart from slight increases between 600–700 hPa in the HIGH_IH.

Unfortunately, the only other profile information available for southern Africa are a limited number of ozone sonde measurements (at Irene, South Africa (25.9° S, 28.2° E) and Malindi, Kenya (3.0° S, 40.2° E)) which were either not operated during July and August or the measurements stopped at the start of 2006. This emphasises the need for expansion of the network of ozone soundings, initiation of ground-based measurements for (e.g.) CO or the continuation (expansion) of the MOZAIC flight network

ACPD
10, 7507–7552, 2010

within the tropics and especially central and southern Africa. Such measurements can be used to constrain the inter-annual variability in BB emissions from this dominant region, validate large scale models and aid (e.g.) the retrieval of total tropical ozone columns (e.g.) de Laat et al. (2009).

4.2 Comparisons in Equatorial Africa

Figure 6 shows comparisons of the monthly mean profiles of tropospheric O_3 from radio sonde measurements at both Cotonou (6.2° N, 2.2° E) and Nairobi (1.3° S, 36.8° E) against co-located model output for the FULL, NOGUIN and NOSAFR simulations. Both stations are part of the SHADOZ (Southern Hemisphere Additional Ozonesondes) network for the tropics (Thompson et al., 2003). Moreover, both stations are also situated near large urban conurbations, although Cotonou is near the coast and therefore subject to more varying types of circulation whereas Nairobi is much further east and not affected by the same dynamics (see Sect. 5).

The comparisons for Cotonou show that whilst over estimating the surface concentrations, TM4_AMMA has difficulty in simulating the increase in [O_3] observed with height, leading to under predictions of between ~30–40% at altitude levels between 600 hPa and the tropopause. It should be noted however that the measurements of this type have been shown to have an accuracy of ±(5–10)% (e.g. Deshler et al., 2008). The "bulge" observed at Cotonou at ~700 hPa in the monthly mean for August is due to an "extreme" event which occurred on the 13 and 14 August, where between 100–120 ppbv of [O_3] was observed (Thouret et al., 2009). This event was also observed in in-situ aircraft measurements performed in the framework of AMMA (Andréas-Hernández et al., 2009) off the coast above Ghana (~6° N, ~1° W). Previously, Sauvage et al. (2005) have shown that the MOZAIC climatology for Lagos, Nigeria (6.6° N, 3.3° E) exhibits similar incidental increases in the MT suggesting such enhancements are an annually recurring phenomenon during the WAM. These authours concluded that although such enhancements are sporadic in nature (i.e.) not continuous throughout the whole of August, such events also exhibit a degree of inter-annual

ACPD
10, 7507–7552, 2010

variability, where measurements taken in different years have observed increases in MT O_3 in 28–45% of cases during the WAM (Sauvage et al., 2007). For 2006 intra-seasonal variability is also seen when examining individual soundings throughout August 2006 (Thouret et al., 2009). This suggests that the transport pathways into the region change markedly on a daily basis as identified for 2006 by Mari et al. (2008).

The enhancement event of 13–14 August 2006 is not captured well by TM4_AMMA. Rather, the maximum [O_3] values due to BB in southern Africa occurred further south (c.f. Fig. 3). Comparing the NOGUIN profile at Cotonou with the observations shows that the effect of BB activity between 0–10° N on the tropospheric O_3 profile is insignificant during the WAM, whereas comparing the corresponding NOSAFR profile shows there is a reduction in tropospheric [O_3] below 800 hPa of ~30–40%. This indicates that the transport determined by the ECMWF meteorology does not introduce polluted air from southern Africa directly into the MT at this latitude but rather into the LT, as shown in Fig. 4. To examine the origin of air reaching the Cotonou site on these extreme days in more detail we performed back-trajectory simulations which are presented in Sect. 5. Finally, an additional comparison was again performed against output from the TM5 model using the configuration described in Sect 4.1. No significant improvement in the quality of the comparison at Cotonou occurred in the MT (V. Huijnen, personal communication, 2009) again indicating that the deficiency in transport in TM4_AMMA is not due to abrupt changes in circulation which are missed as a result of using 6 hourly meteorological fields.

The comparisons for Nairobi show that the monthly mean model profiles agree better with the measurements for this location, especially for July and August in the LT to MT. This is in spite of the sampling frequency at the location being lower than at Cotonou for this season. However, the variability in the monthly mean profile is also much lower than at Cotonou as shown by comparing the magnitude of the 1-σ variability of the means for both sites. This has also been observed in the MOZAIC climatology when comparing the monthly means taken from Lagos and Nairobi (Sauvage et al., 2005). Interestingly, the largest increase in O_3 during August occurs much higher up in

the troposphere, between 300–400 hPa, suggesting an intrusion of air rich in O_3 from the subtropical jet stream (e.g. Zachariasse et al., 2000). There is also a separate peak in the LT around 700 hPa. Comparing the NOSAFR profile reveals that the effect of regional BB close to the launch site is insignificant when adopting the GFEDv2 emission inventory. This provides at least some confidence that TM4_AMMA does not exhibit an underestimation in LT [O_3] in East Africa similar to that found at Cotonou.

Comparing the FULL_8day, HIGH_IH and HIGH_CO simulations at both measurement sites reveals no significant improvement in model performance (not shown), even though the location of the Nairobi sounding is within the SH. For Cotonou this is due to the differences not being seen as far north as the measurement site. Similar comparisons for the HIGH_ANTH run (not shown) only shows increases in O_3 of a few percent in the lowest kilometer which agrees with the conclusions of Sauvage et al. (2007) related to MOZAIC profiles taken in July at Lagos, Nigeria (6.6° N, 3.3° E) during 2003.

The top panels of Fig. 7 show comparisons of tropospheric CO and O_3 measured in-situ on board of the BAe-146 aircraft during a flight on 13 August 2006, with co-located model output and the altitude at which the measurements were made. The bottom panels show the corresponding flight track of the aircraft, where a colour scale is provided to show the location where the extreme events in each respective trace gas occurred. It can be seen that during this day the aircraft encountered an air mass with very high [CO] and [O_3] near the coast at about 8h50 on the southward flight segment (at ~3.5 km) and at about 10:00 h on the return northward flight segment (at ~2.5 km). These plumes were encountered at similar altitudes to where the maximum [O_3] was seen in the sondes, and thus suggest the same source. The large concentrations in both species suggest an aged BB plume, where the photochemical production of O_3 has formed over previous days (Jost et al., 2003). Moreover, corresponding acetonitrile measurements, which act as a "marker" for BB, also show associated increases (Reeves et al., 2010). All of the sensitivity runs fail to capture this enhancement except the NOSAFR run, whose relative increases are of the order of ~10–20% compared to the ~200–300% increases observed. For the majority of sensitivity studies there

appears to be an anti-correlation for both CO and O_3 between the model and measurements during these enhancement events.

For locations further inland, e.g. before 9h and after 10:15 h , there is an anti-correlation between CO and O_3 in the observations. The corresponding acetonitrile signature is low (not shown) indicating air-masses which are more representative of the background. Here, the agreement of all simulations with the observations becomes much better, especially for O_3. Again, the exception is the NOSAFR simulation, which shows that southern BB has a large influence on the tropospheric background between 8–10° N and introduces the most variability with respect to CO, contributing between ~30–80% of [CO] simulated in the FULL run. This is in spite of the weak northerly transport shown in Fig. 3. For [O_3] the contribution from southern BB is typically ~20–30%, this reduction is partly due to less transport of ozone pre-cursors such as PAN into the region (not shown). For most of the other runs shown the model generally over-predicts [O_3] whenever the aircraft is at low altitude. One possible reason is the under-estimation in dry deposition over vegetated areas, which has been shown for TM4_AMMA in previous studies (Williams et al., 2009a).

Figure 8 shows a corresponding comparison for the measurements taken on the 14 August. Comparing the location of the flight tracks it can be seen that the flight path is quite similar to that of the 13 August, apart from the latitudinal range covered. Moreover, the background [CO] and [O_3] are also similar, where an anti-correlation between CO and O_3 in the measurements is again quite evident. The agreement for each of the trace species is consistent with that shown for similar locations in Fig. 7 in that the [O_3] is higher by ~100% in the model. Again the NOSAFR simulation seems to reproduce much of the large scale variability in O_3, albeit with a smaller amplitude, i.e. the broad peaks at 05:00 h, 07:30 h and 08:40 h, which correspond with measurements made between 2–3 km. This suggests either the photochemical processing of the plume maybe insufficient in the CTM or that the timing and/or emission flux of the GFEDv2 biomass burning inventory in the NH is not optimal.

When comparing the other sensitivity studies it can be seen that for the FULL_8day

and NOGUIN runs there is no significant improvement, as seen for the MOZAIC comparisons shown in Fig. 5 and the ozone sonde comparisons shown in Fig. 6. For the HIGH_CO run (not shown) there is a significant degradation in the quality of the comparisons with respect to CO, as a result of the background increasing ~50ppbv.

5 Trajectory calculations

The extreme events seen during August in both the sonde and aircraft measurements near the southern coast of West Africa suggest an air mass that has been in recent contact with BB emissions (similar to that suggested in Andréas-Hernández et al., 2009). However, we have shown that the northward transport of polluted air from southern Africa is constrained to ~2–4° N for the MT in TM4_AMMA (c.f. Fig. 3), even though the model captures the "break" phase in northward transport (Mari et al., 2008). One governing factor related to the long-range transport of polluted plumes is the ECMWF meteorological analysis data which are used to drive the CTM. An independent way to check if the ECMWF operational analysis describes the large scale transport correctly is to calculate trajectories, whose origins are instructive as to what causes the underestimation in the CTM. Here we present a number of 10-day trajectory calculations initiated (a) in the region where the most intense BB activity occurs during August, (b) around the location at which the ozone soundings were launched and (c) along the aircraft flight paths shown in the preceding sections. For this purpose we applied the TRAJKS trajectory model (Scheele et al., 1996), which uses the same 6 hourly ECMWF operational dataset as that used to drive TM4_AMMA, except at a 0.5°×0.5° resolution and compares favorably with other trajectory models (Stohl et al., 2001).

Figure 9a–c shows the strength and distribution of CO emissions from Africa during August 2006 as given in the monthly GFEDv2 inventory, along with 10-day forward trajectory calculations initiated on the 4 August at ~800 hPa and finishing on the 14 August. The end date corresponds with the date on which the "extreme" event was observed. The bulk trajectories are placed in the latitude range of 10–15° S between

15–20° E and 25–30° E, respectively, with both being initiated 1.5 km above the ground to account for rapid convective uplift of (e.g.) CO. From Fig. 9b it can be seen that once the air masses travel westwards they loose altitude and travel through the LT towards the north-west. Although some do reach the southern coast of West Africa they are at a much lower altitude than the "peak" which is observed at ~650 hPa. This explains the NOSAFR profile shown in Figs. 4 and 6. Fig. 9c shows that the BB which occurs in Central Africa is transported northwards and lifted by convective mixing towards the equator as found in Barret et al. (2008). Additional trajectories initiated for various days during August between 0–5° S and 10–20° E (not shown) all follow a north-easterly direction. Therefore, the ECMWF meteorology predicts that air-masses which originate near regions exhibiting BB do not travel directly into the MT around 6° N.

Figure 10a and b show 10-day back trajectory calculations starting on 3 and 14 August at ~600 hPa from the Cotonou measurement site (i.e.) where elevated [O_3] was measured. These dates correspond to ozone sonde measurements that give profiles both with (14 August) and without (3 August) an enhancement in MT O_3 (Mari et al., 2008; Thouret et al., 2009). It can be seen that there are distinct differences between the air mass histories on these two days. For the 3 August the air at this altitude originates from either the LT in the Gulf of Guinea or from the Saharan region to the north. For the 14 August the air at ~600 hPa originates to the west of the measurement site, where it passes over eastern Nigeria a few days prior to reaching Cotonou. This suggests that the enhanced MT O_3 observed in the sondes is due to the northerly transport of BB polluted plumes over the Gulf of Guinea which are present in the MOPITT composite (Mari et al., 2008) but not captured in the model (c.f. Fig. 3).

Figures 11a and b show the corresponding 10-day back trajectories initiated on the 13 August along the flight path of the BAe-146 aircraft at the 9 h and 10 h, respectively (c.f. Fig. 7). It can be seen clearly that, again, the air circles the region anti-cyclonically for a few days preceding the measurement. Again, when considering the large [CO] observed in the MOPITT composite (Mari et al., 2008), the yellow pressure contours show that the height at which the air-masses reside coincides with highly polluted air-masses

a few days before the measurement. Similar back trajectory calculations performed by Andréas-Hernández et al. (2009) have shown that polluted air sampled by the DLR aircraft originate from the MT (~500 hPa) to the west over Cameroon. Back trajectories performed for the flight shown in Fig. 8 (not shown) reveal that in this case the air predominantly originates from the LT in North Africa, gradually rising as it travels south west passing over the Sahel and Saharan regions (not shown), resulting in [CO] and [O_3] which are representative of the background. The signature in O_3 in the NOSAFR run corresponds with measurements taken at higher altitudes where the effect of deposition becomes less important. Moreover, such an event is also not present in the alternative L3JRCv2 inventory of Liousse et al. (2004), which has been used for both global CTM simulations during 2006 (Williams et al., 2010) and meso-scale transport studies (Real et al., 2009).

Finally, we also performed the trajectories shown in Figs. 9–11 using the meteorological dataset available for August 2006 which have assimilated the AMMA radio soundings (Agusti-Panareda et al., 2009). There is a strong impact on including the new measurements on the location of the AEJ in the ECMWF analysis. The trajectory results presented here show that the inclusion of the additional measurements leads to significant differences in the origin of the trajectories. For brevity we do not show all the corresponding trajectories here but only those which exhibit the most interesting differences. Figure 12 shows the corresponding backward trajectories as those shown in Fig. 10b (from Cotonou on the 14 August) and 11a (from the BAe-146 flight path at 09:00 h on 13 August) using the updated meteorological fields. For the Cotonou sounding the origin of the air-mass is either directly from southern Africa or the LT of the Atlantic Ocean, which we have shown to be affected by westerly transport of BB plumes (Fig. 4). For the BAe-146 flight, the air circulates in the same direction as that shown in Fig 11a and passes nearer Cameroon, therefore near the region where the BB plumes are transported northwards inland (c.f. Fig. 9c). Moreover, the forward trajectory calculations corresponding to Fig. 9b and c (not shown) indicate more trajectories impinging on the coast (albeit in the LT) and more trajectories from Central

Africa passing between ~5–6° N around 500–600 hPa. This implies that the quality of the CTM simulations would improve if adopting the new meteorological dataset and also shows the limitations in using trajectory studies in EA in order to explain observations without corresponding chemical signatures (such as elevations in acetonitrile).

6 Conclusions

In this study we have investigated the influence that regional biomass burning emissions from southern and northern Africa have on the composition of the lower troposphere over Equatorial Africa during the West African Monsoon in 2006. By performing a set of sensitivity studies we have shown that emissions from southern Africa dominate tropospheric composition over the Equatorial Atlantic for this season, and influence a large area in the Northern Hemisphere upto ~15° N. When using the GFEDv2 biomass burning emission inventory and 6 hourly ECMWF meteorological fields, the maximum concentrations of [CO] and [O_3] occur between 0–5° S during August, which is more southerly than the distribution observed in satellite measurements. This behaviour has also been previously seen when adopting the alternative L3JRCv2 emission inventory by Liousse et al. (2004) in a number of different chemistry transport models (Williams et al., 2009a).

By varying both the temporal distribution and injection heights at which emissions are introduced we have shown that, although there is little effect near the source regions, temporal variability has a larger effect than the choice of injection height on tropospheric [O_3] and [CO] in the outflow regions over the Gulf of Guinea. This finding agrees with the conclusions of the study of Chen et al. (2009) concerning northern boreal fires, providing further evidence that, when available, weekly variation in biomass burning activity should be included in preference to monthly averages when performing large-scale modeling studies aimed at investigating tropical pollution events and the seasonal composition of the tropical troposphere.

For tropospheric CO comparisons of co-located model output against MOZAIC mea-

surements taken during June-July-August we have shown that the model underestimates concentrations near the main source regions. Corresponding comparisons made with AMMA flight data over Equatorial Africa show that further away from the main biomass burning emission source the model tends to over-estimate the background [CO]. Sensitivity tests where the CO flux from biomass burning in southern Africa was increased by 50% are somewhat inconclusive, in that the improvements seen in the tropospheric profile in the lower troposphere near the source regions cause an associated degradation in the model performance over Equatorial Africa. Thus the disagreement is most likely due to inaccuracies in either a biomass burning event near the airport and/or the temporal distribution of the burning activity in the GFEDv2 emission inventory, an urban emission source close to the airport or missing sources in the model such as enhanced biogenic activity. The under sampling of atmospheric composition for the lower troposphere in southern Africa significantly hinders the assessment of the accuracy of the GFEDv2 emission inventory when applied in a global chemistry transport model.

For tropospheric O_3 the profiles simulated in the model near both the source regions and in East Africa are in fairly good agreement with measurements. For West Africa there is a significant under-estimation for the middle to upper troposphere as compared to ozone sonde profiles. For the background, the model typically over estimates the $[O_3]$ measured by in-situ flight data, similar to that seen for CO.

Finally, using a set of trajectory calculations we have shown that direct transport of polluted plumes from southern Africa affect the lower troposphere below 800 hPa rather than the mid troposphere when driving the model with 6 hourly ECMWF meteorological analyses. Repeating the trajectory studies using a meteorological dataset which assimilates soundings taken during August around the region reveals that the ECMWF fields change markedly when containing the new information. The upgraded dataset shows that direct transport of air from southern Africa into the AMMA measurement region is more probable. Therefore the performance of the CTM is heavily constrained by the accuracy of the meteorological data applied for the region.

ACPD
10, 7507–7552, 2010

Acknowledgements. The authors acknowledge the EU integrated project AMMA (African Monsoon Multidisciplinary Analysis, contract 004089-2) for the support network and funding. Based on a French initiative, AMMA was built by an international scientific group and is currently funded by a large number of agencies, especially from France, the United Kingdom, the United States and Africa. It has been the beneficiary of a major financial contribution from the European Community Sixth Framework Research Programme. Detailed information on scientific co-ordination and funding is available on the AMMA International Web site at www.amma-international.org. JEW also acknowledges the EU integrated project SCOUT-O3 (Stratospheric-Climate links with emphasis On the Upper Troposphere and lower stratosphere, contract 505390-GOCE-CT-2004) for partial funding of this work. We also acknowledge the RETRO (EVK2-CT-2002-00170) EU project for providing the emission inventories used in this study.

References

Agusti-Panareda, A., Beljaars, A., Cardinali, C., Genkova, I., and Thorncroft, C.: Impact of assimilating AMMA soundings on ECMWF analyses and forecasts, Weather Forcast., in press, 2010.

Andreae, M. O. and Merlet, P.: Emission of trace gases and aerosols from biomass burning, Global Biogeochem. Cy., 15(4), 955–966, 2001.

Andrés-Hernàndez, M. D., Kartal, D., Reichert, L., Burrows, J. P., Meyer Arnek, J., Lichtenstern, L., Stock, P., and Schlager, H.: Peroxy radical observtaions over West Africa during AMMA 2006: photochemical activity in the outflow of convective systems, Atmos. Chem. Phys., 9, 3681–3695, 2009, http://www.atmos-chem-phys.net/9/3681/2009/.

Ancellet, G., Leclair de Bellevue, J., Mari, C., Nédélec, P., Kukai, A, Borbon, A., and Perros, P.: Effects of regional-scale and concevtive transports on tropospheric ozone chemsirty revealed by aircraft observations during the wet season of the AMMA campaign, Atmos. Chem. Phys., 9, 383–411, 2009, http://www.atmos-chem-phys.net/9/383/2009/.

Barret, B., Ricaud, P., Mari, C., Attié, J.-L., Bousserez, N., Josse, B., Le Flochmoën, E., Livesey, N. J., Massart, S., Peuch, V.-H., Piacentini, A., Sauvage, B., Thouret, V., and Cammas, J.-P.: Transport pathways of CO in the African upper troposphere during the monsoon season:

a study based upon the assimilation of spaceborne observations, Atmos. Chem. Phys., 8, 3231–3246, 2008, http://www.atmos-chem-phys.net/8/3231/2008/.

Bian, H., Chen, M., Kawa, R., Duncan, B., Arellano, A., and Kasibhatla, K.: Sensitivity of global CO simulations to uncertainties in biomass burning sources, J. Geophys. Res., 112, D23308, doi:10.1029/2007JD008376, 2007.

Boersma, K. F., Jacob, D. J., Eskes, H. J., Pinder, R. W., Wang, J., and van der A, R. J., Intercomparison of SCIAMACHY and OMI tropospheric NO2 columns: Observing the diurnal evolution of chemistry and emissions from space, J. Geophys. Res., 113, D16S26, doi:10.1029/2007JD008816, 2008.

Chen, Y, Li, Q., Randerson, J. T., Lyons, E. A., Kahn, R. A., Nelson, D. L. and Diner, D. J.: The sensitivity of CO and aerosol transport to the, temporal and vertical distribution of North American boreal fire emissions, Atmos. Chem. Phys., 9, 6659–6580, 2009, http://www.atmos-chem-phys.net/9/6659/2009/.

Colarco, P. R., Schoberl, M. R., Dodderidge, B. G., Marufu, L. T., Torres, O., and Welton, E. J.: Transport of smoke from Canadian forest fires to the surface near Washington, D. C.: Injection height, entrainment, and optical properties, J. Geophys. Res., 109, D06203, doi:10.1029/2003JD004248, 2004.

Crutzen, P. J. and Andreae, M. O.: Biomass burning in the tropics: Impact on atmospheric chemistry and biogeochemical cycles, Science, 250, 1669–1678, 1990.

de Laat, A. T. J., Gloudemans, A. M. S., Schrijver, H., van den Broek, M. M. P., Meirink, J. F., Aben, I., and Krol, M.: Quantitative analysis of SCIAMACHY carbon monoxide total column measurements, Geophys. Res. Lett., 33, L07807, doi:10.1029/2005GL025530, 2006.

de Laat, A. T. J., van der A, R. J., and van Weele, M.: Evaluation of tropospheric ozone columns derived from assimilated GOME ozone profile observations, Atmos. Chem. Phys., 9, 8105–8120, 2009, http://www.atmos-chem-phys.net/9/8105/2009/.

Deshler, T., Mercer,. J., Smit, H. G. J., et al.: Atmospheric comparison of electrochemical cell ozonesoundes from different manufacturers, and with different cathode solution strengths: The Balloon Experiment on Standards for Ozone sondes, J. Geophys. Res., 113, D04307, doi:10.1029/2007JD008975, 2008.

Edwards, D. P., Emmons, L. K., Gille, J. C., Chu, A., Attie, J.-L., Giglio, L., Wood, S. W., Haywood, J., Deeter, M. N., Massie, S. T., Ziskin, D. C., and Drummond, J. R.: Satellite-observed pollution from Southern Hemisphere biomass burning, J. Geophys. Res., 111, D14312, doi:10.1029/2005JD006655, 2006.

Fu, Q.: An accurate parameterization of the solar radiative properties of cirrus clouds for climate models, J. Climate, 9, 2058–2082, 1996.
Giglio, L.: Characterization of tropical diurnal fire cycle using VIRS and MODIS observations, Remote Sens. Environ., 108, 407–421, 2007.
Giglio, L., Csiszar, I., and Justice, C. O.: Global distribution and seasonality of active fires as observed with Terra and Aqua Moderate Resolution Imaging Spectroradiometers (MODIS) sensors, J. Geophys. Res., 111, G02016, doi:10.1029/2005JG000142, 2006.
Heymsfield, A. J. and McFarquhar, G. M.: High albedos of cirrus in the tropical pacific warm pool: Microphysical interpretations from CEPEX and from Kwajalein, Marshall Islands, J. Atmos. Sci., 53, 2424–2451, 1996.
Heymsfield, A. J.: Properties of Tropical and Midlatitude Ice Cloud Particle Ensembles. Part II: Applications for Mesoscale and Climate Models, J. Atmos. Sci., 60, 2592–2611, 2003.
Hobbs, P. V., Sinha, P., Yokelson, R. J., Christian, T. J., Blake, D. R., Gao, S., Kirchstetter, T. W., Novakov, T., and Pilewskie, P.: Evolution of gases and particles from a savanna fire in South Africa, J. Geophys. Res., 108(D13), 8485, doi:10.1029/2002JD002352, 2003.
Houweling, S., Dentener, F. J., and Lelieveld, J.: The impact of non-methane hydrocarbon compounds on tropospheric photochemistry, J. Geophys. Res., 103(D9), 10673–10696, 1998.
Ito, A and Penner, J. E.: Estimates of CO emissions from open biomass burning in southern Africa for the year 2000, J. Geophys. Res., 110, D19306, doi:10.1029/2004JD005347, 2005.
Intergovernmental Panel for Climate Change, 2007 WGI Climate Change The physical science basis, Contribution of Working Group I to the Fourth Assessment Report of the Intergovernmental Panel on Climate Change, edited by: Solomon, S., Qin, D., Manning, M., Chen, Z., Marquis, M., Averyt, K. B., Tignore, M. and Miller, H. L., Cambridge University Press, Cambridge, UK, 996 pp., 2007.
Jacob, D. J.: Heterogeneous chemistry and tropospheric ozone, Atmos. Enviro., 34, 2131–2159, 2000.
Jain, A. K.: Global estimation of CO emissions using three sets of satellite data for burned area, Atmos. Enviro., 41, 6931–6940, 2007.
Janicot, S., Thorncrof, C. D., Ali, A., and 24 others: Large-scale overview of the summer monsoon over West Africa during the AMMA field experiment in 2006, Ann. Geophys., 26, 2569–2595, 2008, http://www.ann-geophys.net/26/2569/2008/.
Jost, C., Trentmann, J., Sprung, D., Andreae, M. O., McQuaid, J. B., and Barjat, H.: Trace gas chemistry in a young biomass burning plume over Namibia: Observations and model

simulations, J. Geophys. Res., 108, 8482, doi:10.1029/2002JD002431, 2003.
Kahn, R. A., Li, W.-H., Moroney, C., Diner, D. J., Martonchik, J. V., and Fishbein, E.: Aerosol source plume physical characteristics from space-based multiangle imaging, J. Geophys. Res., 112, D11205, doi:10.1029/2006JD007647, 2007.
Krol, M. C., Houweling, S., Bregman, B., van den Broek, M., Segers, A., van Velthoven, P., Peters, W., Dentener, F., and Bergamaschi, P.: The two-way nested global chemistry-transport zoom model TM5: algorithm and applications, Atmos. Chem. Phys., 5, 417–432, 2005, http://www.atmos-chem-phys.net/5/417/2005/.
Labonne, M., Breon F.-M., and Chevallier, F.: Injection height of biomass burning aerosols as seen from a spaceborne lidar, Geophys. Res. Lett., 34, L11806, doi:10.1029/2007GL029311, 2007.
Leung, F.-Y., T., Logan, J. A., Park, R., Hyer, E., Kasischke, E., Streets, D., and Yurganov, L.: Impact of enhanced biomass burning in the boreal forests in 1998 on tropospheric chemistry and the sensitivity of model results to the injection height of emissions, J. Geophys. Res., 112, D10313, doi:10.1029/2006JD008132, 2007.
Liousse, C., Andreae, M. O., Artaxo, P., Barbosa, P., Cachier, H., Gregorie, J. M., Hobbs, P., Lavoue, D., Mouillot, F., Penner, J., and Scholes, M.: Deriving global quantitative estimates for spatial and temporal distributions of biomass buring emissions, in: Emissions of atmospheric trace compounds, edited by: Granier, C., P. Artaxo and C. Reeves, Kluwer Academic Publishers, Dordrecht, The Netherlands, 544 pp., 2004.
Mari, C. H., Cailley, G., Corre, L., Saunois, M., Attié, J. L., Thouret, V., and Stohl, A.: Tracing biomass burning plumes from the Southern Hemisphere during the AMMA 2006 wet season experiment, Atmos. Chem. Phys., 9, 3951–3961, 2008, http://www.atmos-chem-phys.net/9/3951/2008/.
Monks, P. S., Granier, C., Fuzzi, S., Stohl, A., and 59 others: Atmospheric composition change – global and regional air quality, Atmos. Environ., 43, 5268–5350, 2009.
Muhle, J., Brenninkmeijer, C. A. M., Rhee, T. S., Slemr, F., Oram, D. E., Penkett, S. A., and Zahn, A.: Biomass burning and fossil fuel signatures in the upper troposphere observed during a CARIBIC flight from Namibia to Germany, Geophys. Res. Lett., 29(9), 1910, doi:10.1029/2002GL015764, 2002.
Nicholson, S. E., and Grist, J. P.: The Seasonal Evolution of the Atmospheric Circulation over West Africa and Equatorial Africa, J. Clim., 16, 1013–1030, 2003.
Real, E., Orlandi, E., Law, K. S., Fierli, F., Josset, D., Cairo, F., Schlager, H., Borrmann, S.,

Kunkel, D., Volk, M., McQuaid, J. B., Stewart, D. J., Lee, J., Lewis, A., Hopkins, J. R., Ravegnani, F., Ulanovski, A., and Liousse, C.: Cross-hemispheric transport of African biomass burning pollutants: implications for downwind ozone production, Atmos. Chem. Phys. Diss., 9, 17385–17427, 2009.

Redelspeger, J. L., Thorncroft, C. D., Diedhiou, A., Lebel, T., Parker, D. J., and Polcher, J.: African Monsoon Multidisiplinary Analysis – An international research project and field campaign, B. Am. Meteorol. Soc., 87, 1739–1746, 2006.

Reeves, C. E., Formentl, P., Aflf, C. and 26 others: Chemical and aerosol characterization of the troposphere over West Africa during the monsoon period as part of AMMA, Atmos. Chem. Phys. Diss., 10, 7115–7183, 2010.

Roberts, G., Wooster, M. J., and Lagoudakis, E.: Annual and diurnal African biomass burning temporal dynamics, Biogeosciences, 6, 849–866, 2009, http://www.biogeosciences.net/6/849/2009/.

Sauvage, B., Thouret, V., Cammas, J.-P., Gheusi, F., Athier, G., and Nédélec, P.: Tropospheric ozone over Equatorial Africa: regional aspects from the MOZAIC data, Atmos. Chem. Phys., 5, 311–335, 2005, http://www.atmos-chem-phys.net/5/311/2005/.

Sauvage, B., Thouret, V., Thompson, A. M., Witte, J. C., Cammas, J.-P., Nédélec, P. and Athier, G.: Enhanced view of the "tropical Atlantic ozone paradox" and "zonal wave one" from the in situ MOZAIC and SHADOZ data, J. Geophys. Res., 111, D01301, doi:10.1029/2005JD006241, 2006.

Sauvage, B., Gheusi, F., Thouret, V., Cammas, J.-P., Duron, J., Escobar, J., Mari, C., Mascart, P., and Pont, V.: Medium-range mid-tropospheric transport of ozone and precursors over Africa: two numerical case studies in dry and wet seasons, Atmos. Chem. Phys., 7, 5357–5370, 2007, http://www.atmos-chem-phys.net/7/5357/2007/.

Scheele, M. P., Siegmund, P. C., and van Velthoven, P. F. J.: Sensitivity of trajectories to data resolution and its dependence on the starting point: in or outside a tropopause fold, Meteor.Appl., 3, 267–273, 1996.

Schmitt, C. G. and Heymsfield, A. J.: Total Surface Area Estimates for Individual Ice Particles and Particle Populations,J. Appl. Meteor., 44, 467–474, 2005.

Sinha, P., Jaeglé, L., Hobbs, P. V., and Liang, Q.: Transport and biomass burning emissions from southern Africa, J. Geophys. Res., 109, D20204, doi:10.1029/2004JD005044, 2004.

Staudt, A. C., Jacob, D. J., Logan, J. A., Bachiochi, D., Krishnamurti, T. N., and Poisson, N.: Global chemical model analysis of biomass burning and lightning influences over the South

Pacific in austral spring, J. Geophys. Res., 107(D14), 4200, doi:10.1029/2000JD000296, 2002.
Stevenson, D. S., Dentener, F. J., Schultz, M. G., Ellington, K., and 40 others: Multi-model ensemble simulations of present-day and near-future tropospheric ozone, J. Geophys. Res., 111, D08301, doi:10.1029/2005JD006338, 2006.
Stohl, A., Haimberger, L., Scheele, M. P., and Wernli, H.: An intercomparison of results from three trajectory models, Meteor. Appl., 8, 127–135, 2001.
Thompson, A., Witte, J. C., Oltmans, S. J., Schmidlin, F. J., Logan, J. A., Fuijwara, M., Kirchhoff, V. W. J. H., Posny, F., Coetzee, G. J. R., Hoegger, B., Kawakami, S., Ogawa, T., Fortuin, J. P. F., and Kelder, H. M.: Southern Hemisphere Additional Ozonesondes (SHADOZ) 1998–2000 tropical ozone climatology 2. Tropospheric variability and the zonal wave-one, J. Geophys. Res., 108, 8241, doi:10.1029/2002JD002241, 2003.
Thouret, V., Saunois, M., Minga, A., Mariscal, A., Sauvage, B., Solete, A., Agbangla, D., Nédélec, Mari, C., Reeves, C. E., and Schlager, H.: An overview of two years of ozone radio soundings over Cotonou as part of AMMA, Atmos. Chem Phys., 9, 6157–6174, 2009.
Turquety, S., Logan, J. A., Jacob, D. J., Hudman, R. C., Leung, F-Y., Heald, C. L., Yantosca, M., Wu, S., Emmons, L. K., Edwards, D. P. and Sachse, G. W.: Inventory of boreal fire emissions for North America in 2004: Importance of peat burning and pyroconvective injection, J. Geophys. Res., 112, D12S03, doi:10.1029/2006JD007281, 2007.
Van der A, R. J., Eskes, H. J., Boersma, K. F., van Noije, T. P. C., van Roozendael, M., De Smedt, I., Peters, D. H. M. U., and Meijer, E. W.: Trends, seasonal variability and dominant NOx source derived from a ten year record of NO2 measured from space, J. Geophys. Res., 113, D04302, doi:10.1029/2007JD009021, 2008.
Van der Werf, G. R., Randerson, J. T., Giglio, L., Collatz, G. J., Kasibhatla, P. S., and Arellano Jr, A. F.: Interannual variability in global biomass burning emissions from 1997 to 2004, Atmos. Chem. Phys., 6, 3423–3441, 2006, http://www.atmos-chem-phys.net/6/3423/2006/.
Williams, J. E., Scheele, M. P., van Velthoven, P. F. J., and 10 others: Global Chemistry simulations in the AMMA-Model Intercomparison project, B. Am. Meteorol. Soc., doi:10.1175/2009BAMS2818.1, in press, 2010.
Williams, J. E., Scheele, M. P., van Velthoven, P. F. J., Cammas, J.-P., Thouret, V. and Volz-Thomas., A.: The influence of biogenic emissions from Africa on tropical tropospheric ozone during 2006: a global modeling study, Atmos. Chem. Phys., 9, 5729–5749, 2009a, http://www.atmos-chem-phys.net/9/5729/2009/.

Williams, J. E., van Zadelhoff, G.-J., and Scheele, M. P.: The effect of updating scavenging and conversion rates on cloud droplets and ice particles in the TM global chemistry transport model, KNMI technical report TR-308, 1–45, 2009b.

Zachariasse, M., van Velthoven, P. F. J., Smit, H. G. J., Lelieveld, J., Mandal, T. K., and Kelder, H.: Influence of stratosphere-troposphere exchange on tropospheric ozone over the tropical Indian Ocean during the winter monsoon, J. Geophys. Res. 105, 15403–15416, 2000.

Table 1. Definition of the various sensitivity studies used to examine the extent to which BB emissions from different regions of Africa affect lower tropospheric [CO] and [O_3].

Name of Run	GFEDv2 inventory	Details
FULL	Monthly	All biomass burning emissions active
NOGUIN	Monthly	Biomass burning emissions removed between 0–10° N, 20° W–40° E
NOSAFR	Monthly	Biomass burning emissions removed between 0–40° S, 20° W–40° E
FULL_8day	8-day	All biomass burning emissions active
HIGH_IH	8-day	All biomass burning emissions active. Injection height increased to between 0–4 km above surface, with 50% placed above and below 2 km.
HIGH_CO	8-day	As for FULL_8day except the biomass burning emission flux of CO between 0–40° S, 20° W–40° E is increased by 50%

ACPD
10, 7507–7552, 2010

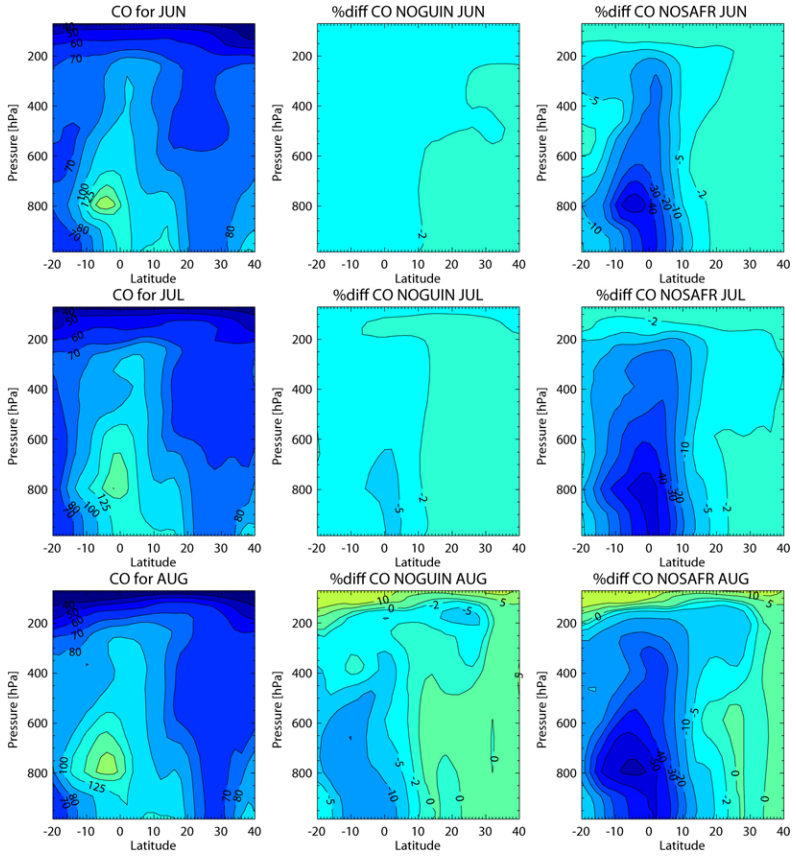

Fig. 1. The influence of regional BB emissions on monthly mean [CO] given in ppbv along the 2-D cross-section taken between 3° W–6° E during June, July and August in 2006. The distribution of tropospheric CO is shown for the FULL simulation (left column) along with the differences for the NOGUIN (middle) and NOSAFR (right) simulations. The differences are calculated for (SENS-FULL)/FULL ×100.

ACPD
10, 7507–7552, 2010

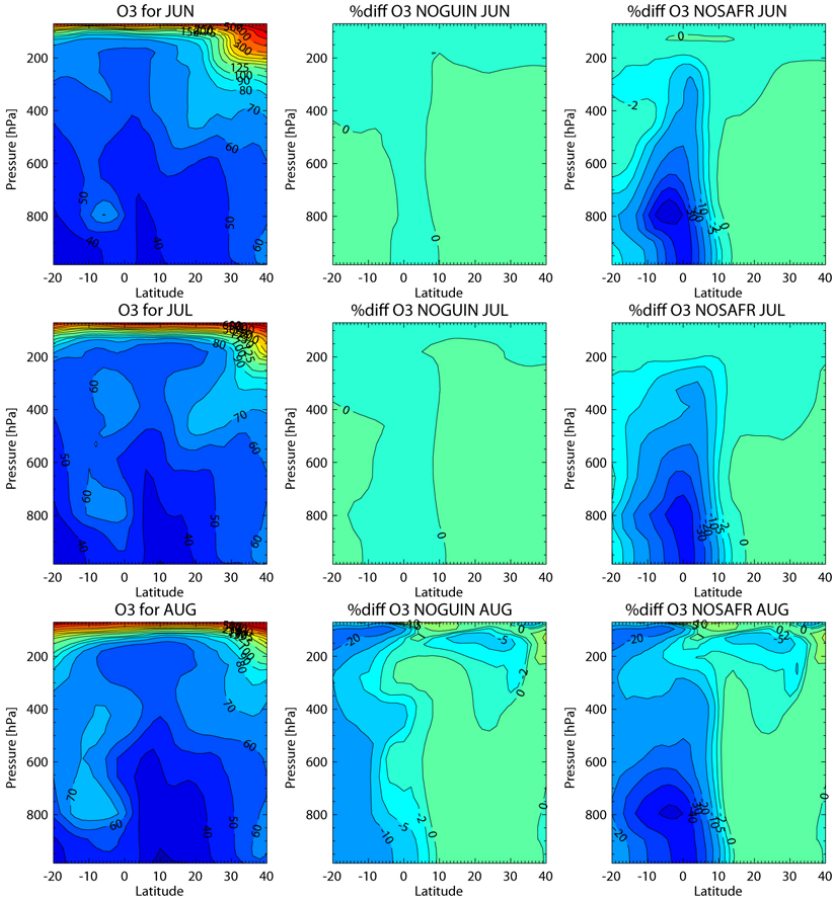

Fig. 2. As for Fig. 1 except for O_3 given in ppbv.

ACPD
10, 7507–7552, 2010

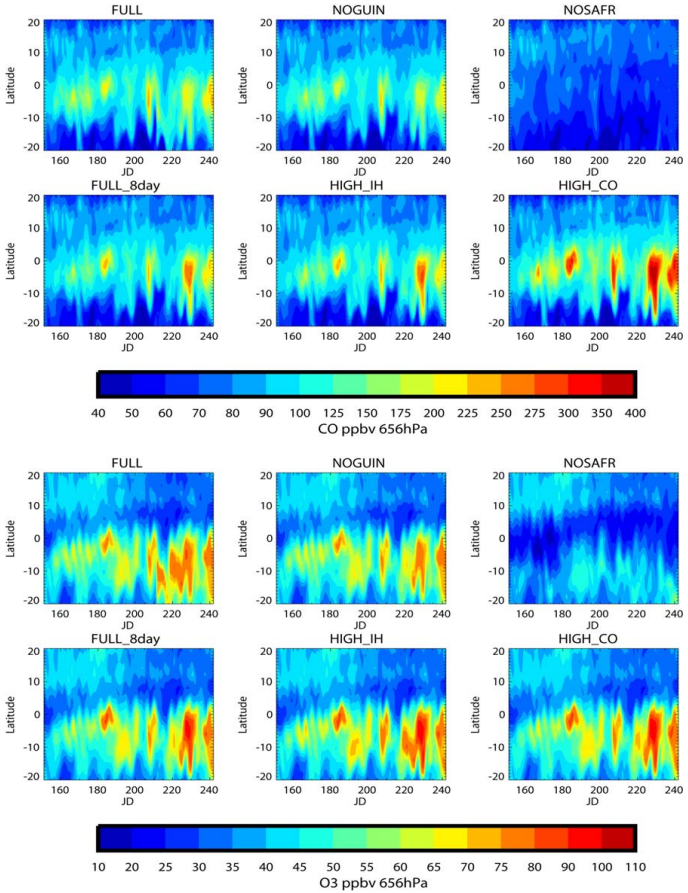

Fig. 3. Hovmöller diagrams of the daily mean for [CO] (top) and [O_3] (bottom) along the 2-D transect averaged between 3° W–6° E. Values are shown for the latitude range 20° S to 20° N during season JJA 2006. The sensitivity tests shown are FULL, NOGUIN, NOSAFR, FULL_8day, HIGH_IH and HIGH_CO. The vertical level shown corresponds to ~650 hPa.

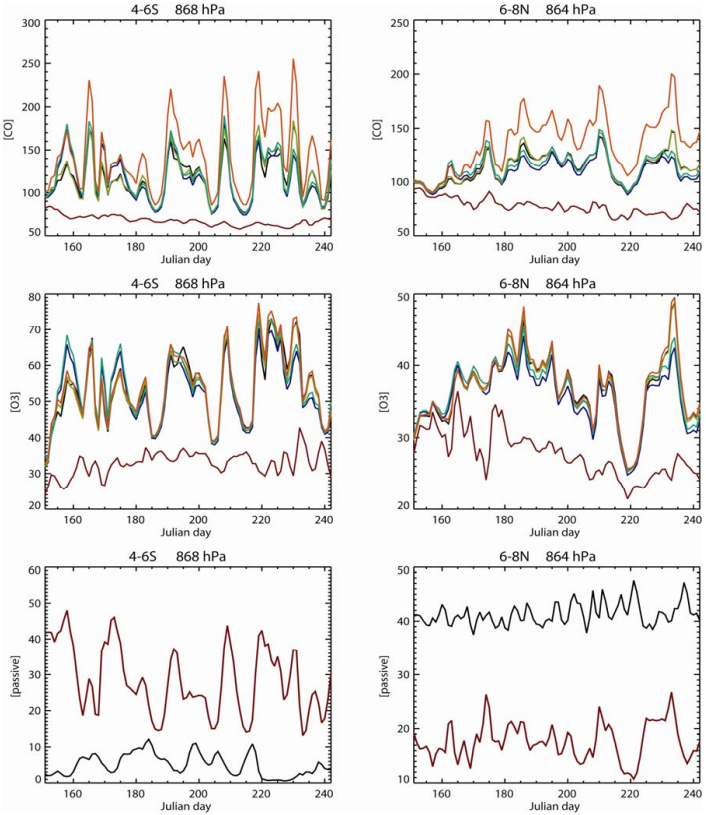

Fig. 4a. Daily mean values of [CO] (top), [O_3] (middle) and the passive tracers (bottom) averaged between 3° W–6° E for season JJA between 4–6° S (left) and 6–8° N (right) at ~860 hPa (~1.5 km height). For the trace gases the colour key is thus; (green) FULL, (blue) NOGUIN, (magenta) NOSAFR, (olive green) FULL_8day, (black) HIGH_IH and (orange) HIGH_CO, given in ppbv. For the passive tracers (black) represents Guinea and (magenta) southern Africa, given in pptv.

ACPD
10, 7507–7552, 2010

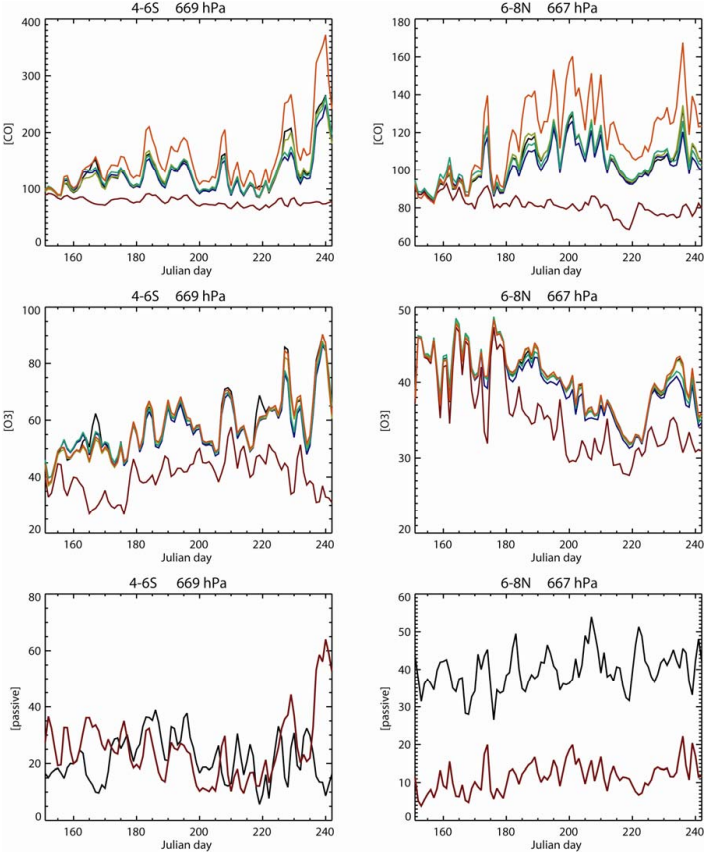

Fig. 4b. Same as Fig. 4a, but at ~670 hPa (~3.3 km height).

ACPD
10, 7507–7552, 2010

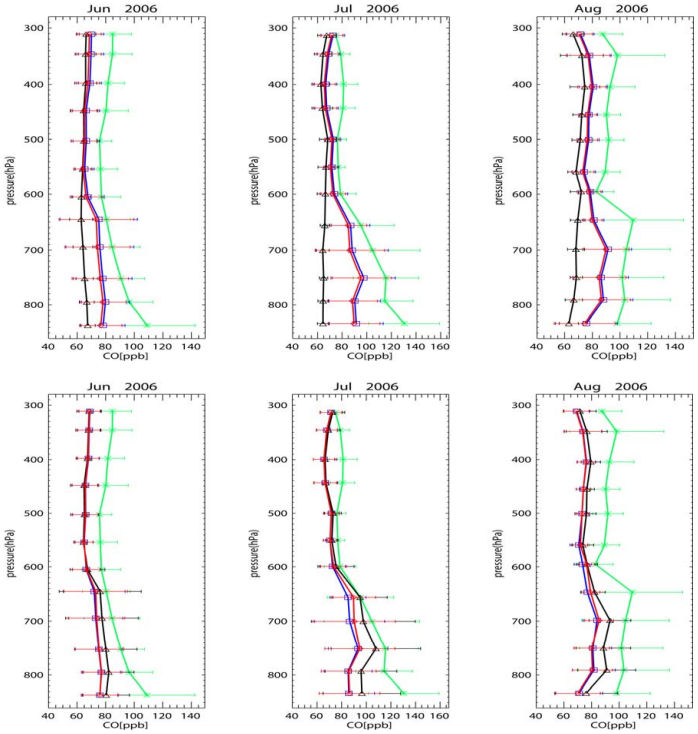

Fig. 5. Comparisons of monthly mean tropospheric profiles for CO taken at Windhoek in Namibia (22.5° S, 17.5° E) against co-located model output from TM4_AMMA for season JJA during 2006. The mean values from the measurements, and their standard deviations, are shown in green. The results of six different simulations are shown. The top row shows: FULL (blue), NOGUIN (red) and NOSAFR (black) simulations. The bottom row shows: simulations using emissions with 8-daily variability: FULL_8day (blue), HIGH_IH (red) and HIGH_CO (black). The error bars represent 1-σ deviation from the mean values.

ACPD
10, 7507–7552, 2010

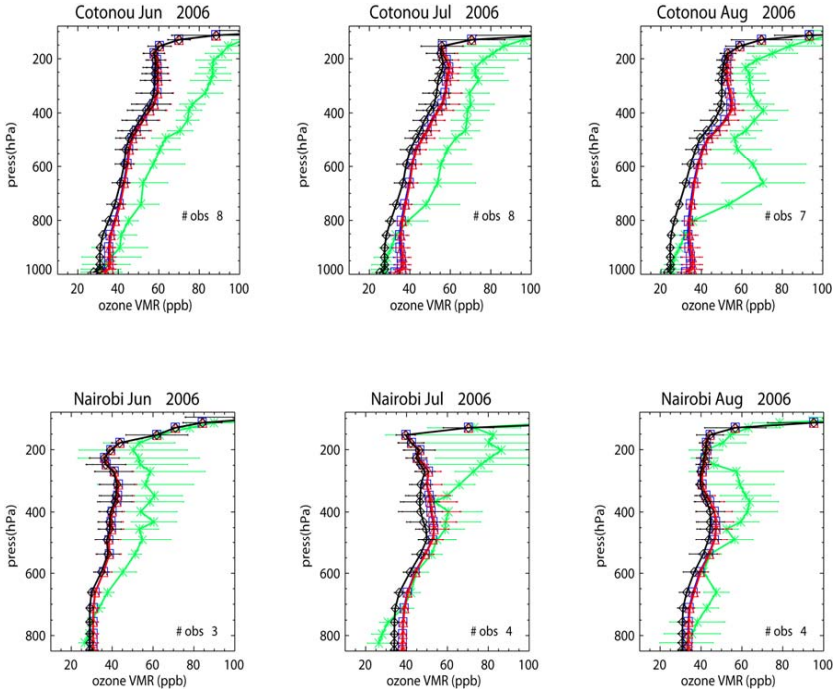

Fig. 6. Comparisons of monthly mean tropospheric radio sonde profiles for O_3 (green lines) taken at Cotonou, Nigeria (6.2° N, 2.2° E) and Nairobi, Kenya (1.3° S, 36.8° E) against co-located model output from TM4_AMMA for month June, July and August 2006. The number of measurements used for calculating each monthly mean are given within each panel. The results of three different simulations are shown: FULL (blue), NOGUIN (red) and NOSAFR (black). The error bars represent 1-σ deviation from the mean.

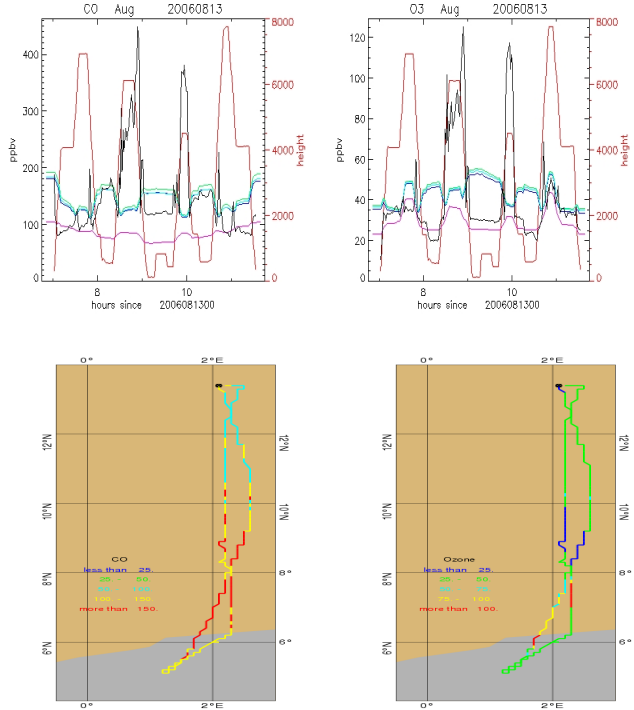

Fig. 7. Top panel: Comparisons of tropospheric CO (left) and O_3 (right) measured on the BAe-146 against TM4_AMMA output for the 13 August 2006. The start/end of the flight is shown as the black dot and the altitude of the aircraft (in m) is shown as the red line. The measurements are indicated by black lines. The results of four different simulations are shown: FULL (green), FULL_8day (cyan), NOGUIN (blue) and NOSAFR (pink). The bottom panels show the flight track of the aircraft with colour coding for the CO (left) and O_3 measurements (right) in ppbv, respectively.

ACPD
10, 7507–7552, 2010

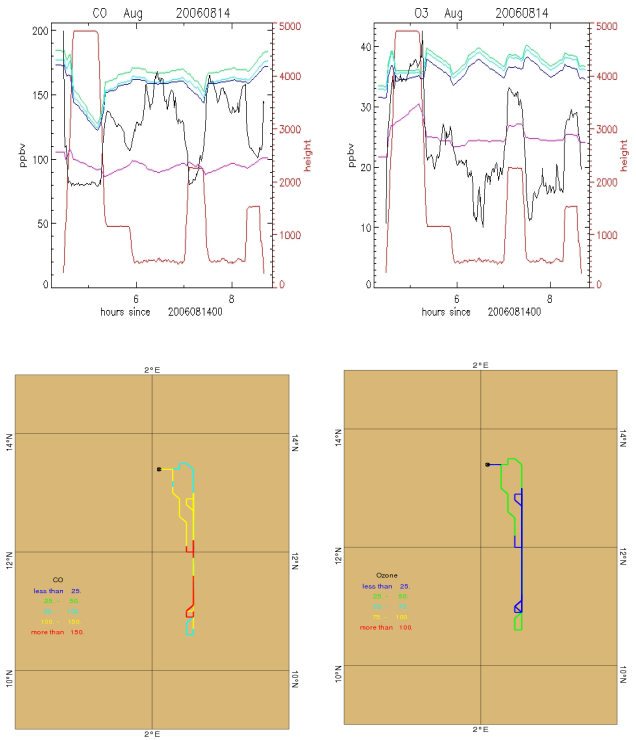

Fig. 8. Comparisons of tropospheric CO (left) and O_3 (right) measured on the BAe-146 against TM4_AMMA output on the 14 August 2006. The altitude of the aircraft is shown as the red line. The colour key is identical to that described for Fig. 7. The bottom panels show the corresponding location of the aircraft for which these measurements occurred.

ACPD
10, 7507–7552, 2010

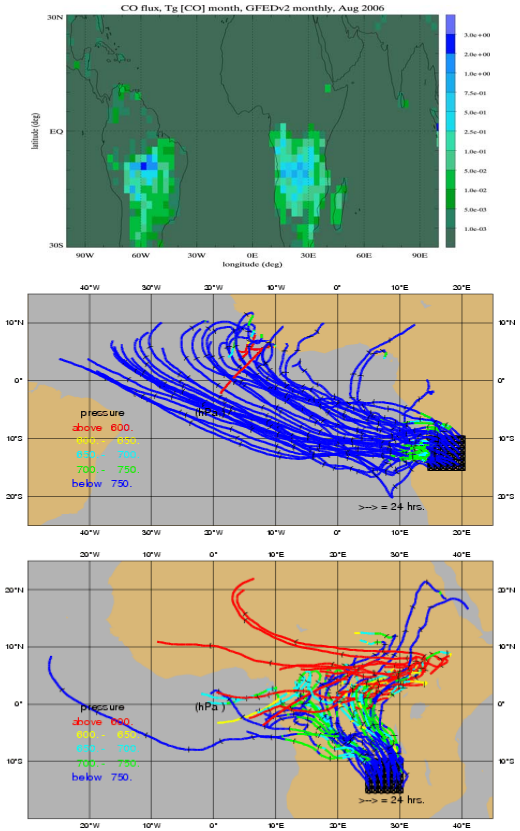

Fig. 9. Ten day forward trajectories starting from two regions exhibiting intense BB activity in the GFEDv2 monthly emission inventory, whose distribution is shown in the top panel **(a)**. Separate trajectories were initiated at a distance of 1° between 10–15° S and (middle, **b**) 15–20° E and (bottom, **c**) 25–30° E on the 4 August 2006. The pressure levels through which each trajectory passes are indicated: >750 hPa (blue), 700–750 hPa (green), 650–700 hPa (cyan), 600–650 hPa (yellow) and <600 hPa

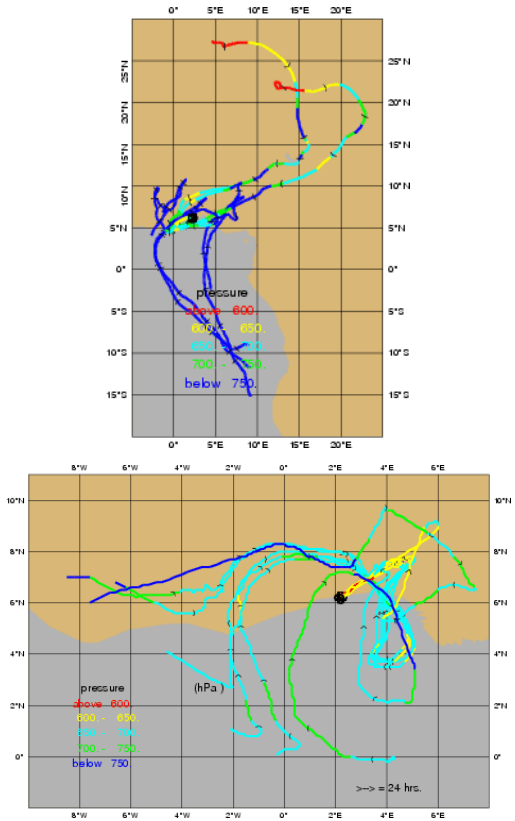

Fig. 10. Ten day back trajectories ending at the Cotonou launch site (6.2° N, 2.2° E) on 3 (top) and 14 August (bottom), 2006. The black arrows indicate one-day time intervals along the back trajectory. The pressure levels through which each trajectory travels are shown using the same colour key as Fig. 9.

ACPD
10, 7507–7552, 2010

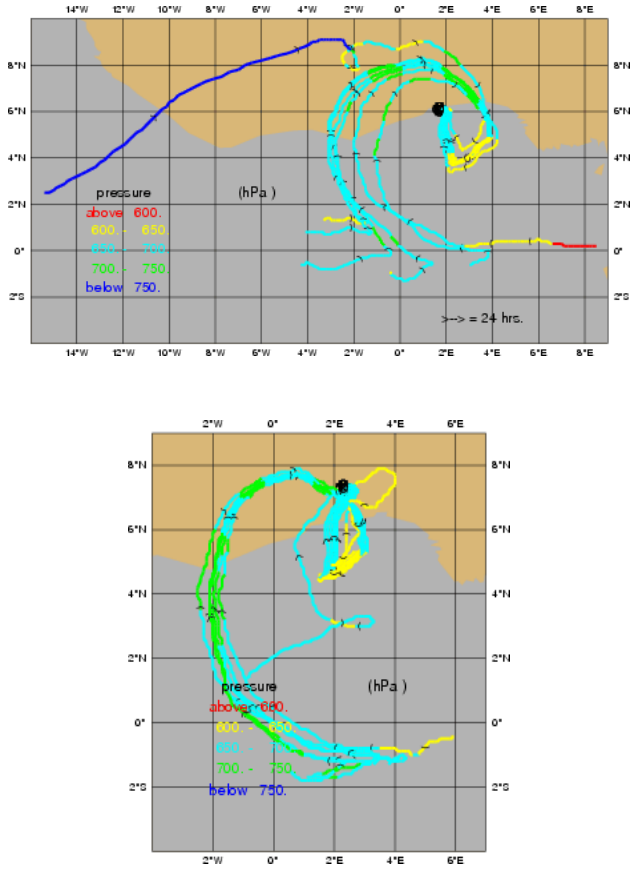

Fig. 11. Ten day back trajectories ending at the location of the BAe-146 aircraft on 13 August at (top) 9 a.m. and (bottom) 10am local time. The black arrows indicate one-day time intervals along the back trajectories. The numbers indicate the pressures at which the air starts and ends (in paranthesis). The colour coding also indicates pressure.The pressure levels through which each trajectory travels are shown using the same colour key as Fig. 9.

ACPD
10, 7507–7552, 2010

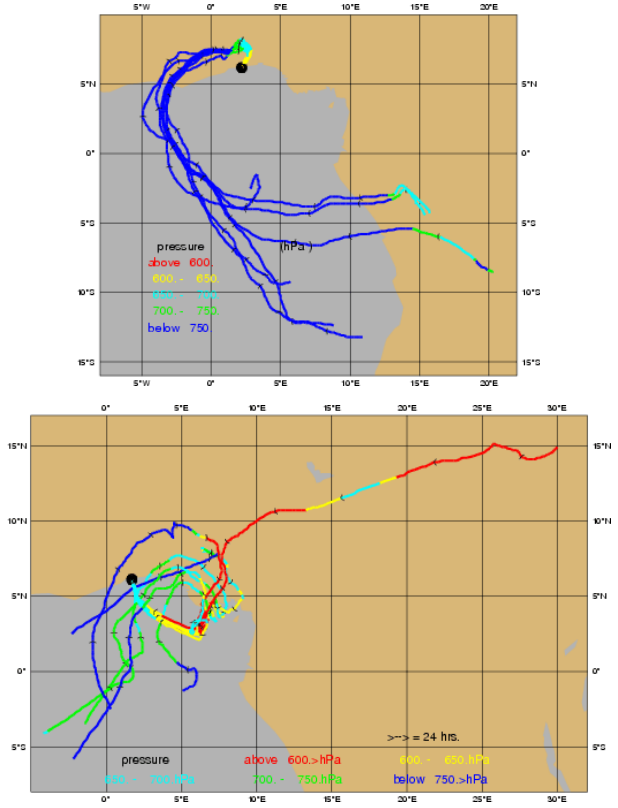

Fig. 12. Ten day back trajectories using the new ECMWF meteorological dataset which assimilates additional sounding information taken during AMMA (Agusti-Panareda et al., 2009). The trajectories shown are (top) for the Cotonou measurement site starting on the 14 August (corresponding with Fig. 10b) and (bottom) for the BAe-146 flight on the 13 August at 9 a.m. local time (corresponding with Fig. 11a).The pressure levels through which each trajectory travels are shown using the same colour key as Fig. 9.

ACPD
10, 7507–7552, 2010